Electronic Supplementary Information For:

Composites of Boron-doped Carbon Nanosheets and Iron Oxide Nanoneedles: Fabrication and Lithium Ion Storage Performance

Yongqiang Yang,[a] Jianan Zhang, [a] Xiaochen Wu, [a] Yongsheng Fu,[b] Haixia Wu [a,*], and Shouwu Guo[a,b,*]

[a]Key Laboratory for Thin Film and Microfabrication of the Ministry of Education, Research Institute of Micro/Nano Science and Technology, Shanghai Jiao Tong University, Shanghai 200240, P. R. China. Tel/Fax: 0086-21-34206915, E-mail: swguo@sjtu.edu.cn, haixiawu@sjtu.edu.cn

[b]School of Materials Science and Engineering, Shaanxi University of Science and Technology, Xi'an, Shaanxi 710021, P. R. China.

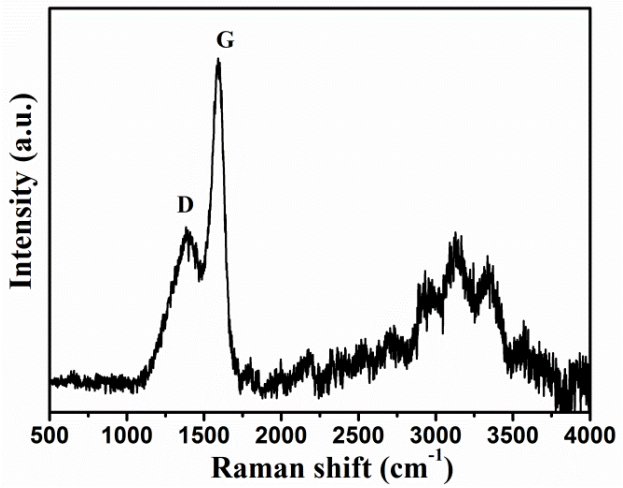

Fig. S1 Raman spectrum of the boron-doped carbon sheets.

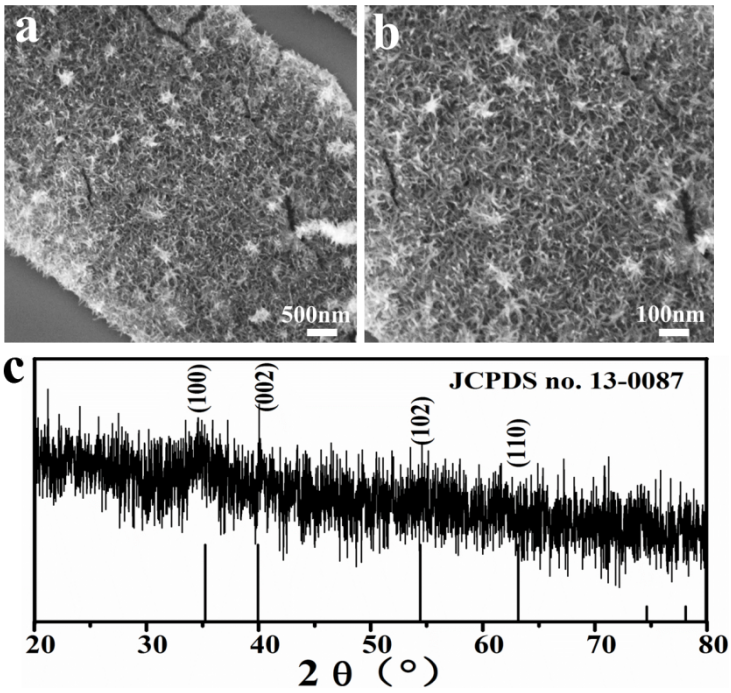

Fig. S2 (a, b) SEM images of the FeOOH/boron-doped carbon nanosheets; (c) XRD pattern of the samples.

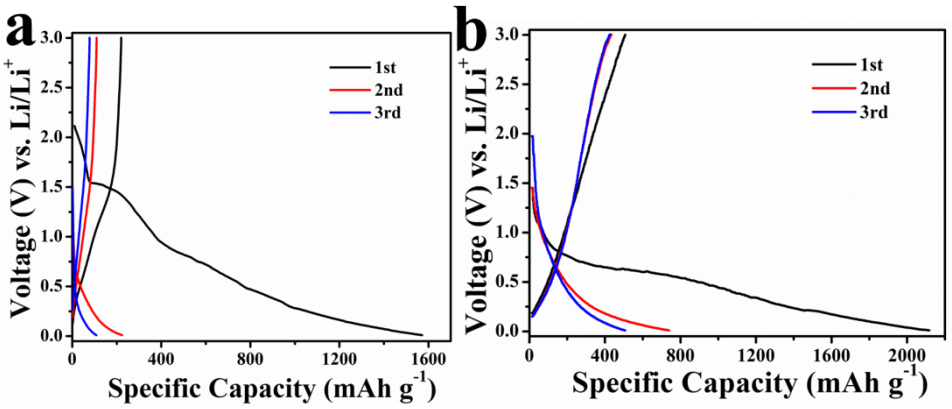

Fig. S3 Discharge-charge voltage profiles of FeOOH/boron-doped carbon nanosheets (a) and boron-doped carbon nanosheets (b) electrode at the 1st, 2nd, and 3rd cycles at a current density of 100 mA g^{-1}.

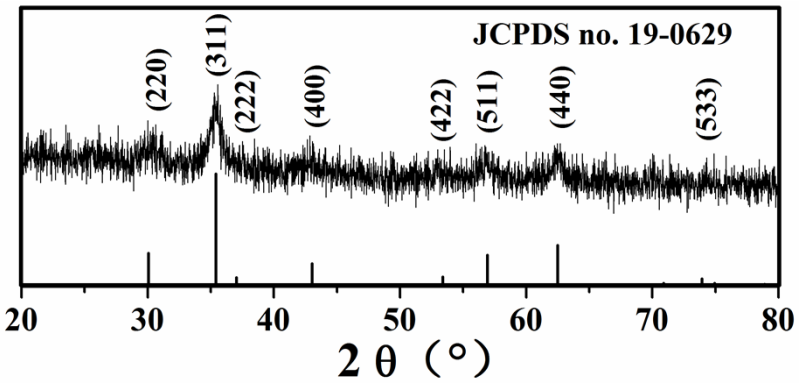

Fig. S4 XRD pattern of the hierarchical boron-doped carbon nanosheets/Fe_3O_4 obtained after being annealed in a nitrogen atmosphere at 350 °C for 2 h.

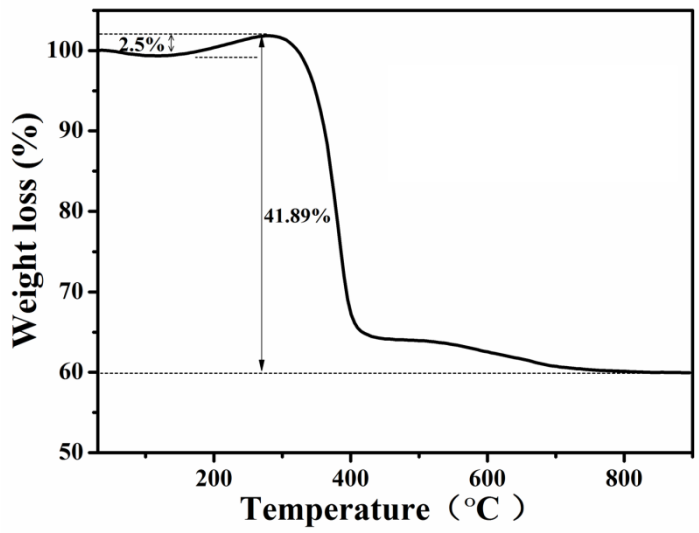

Fig. S5 TGA curve of the composites of boron-doped carbon nanosheets and Fe_3O_4 nanoneedles obtained under air atmosphere.

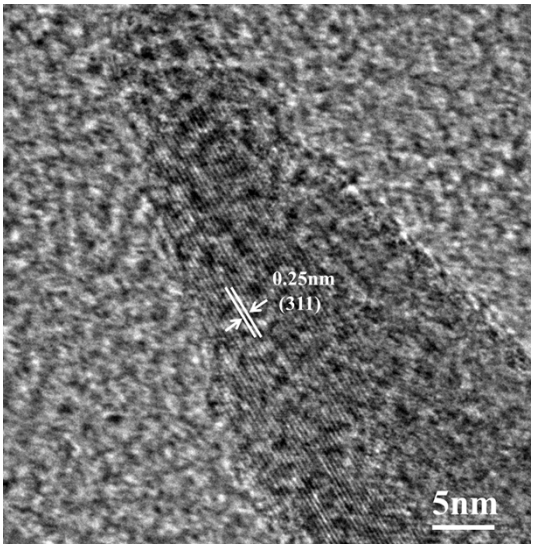

Fig. S6 HRTEM image of Fe_3O_4 nanoneedle.

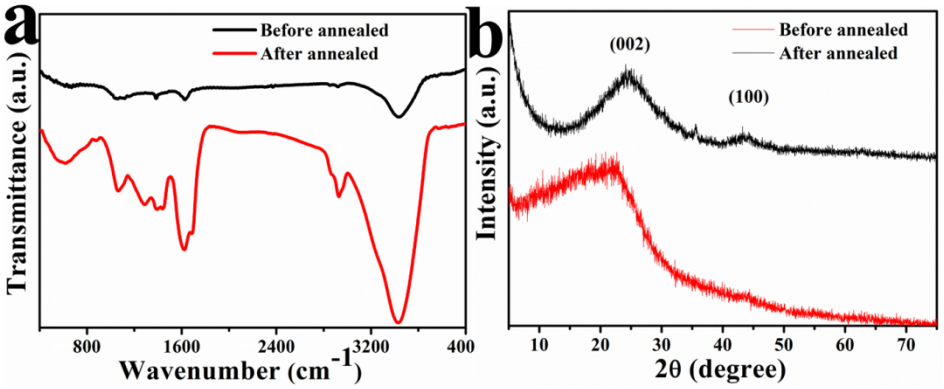

Fig. S7 FT-IR (a) and XRD (b) spectrum of the boron-doped carbon nanosheets before/after annealing.

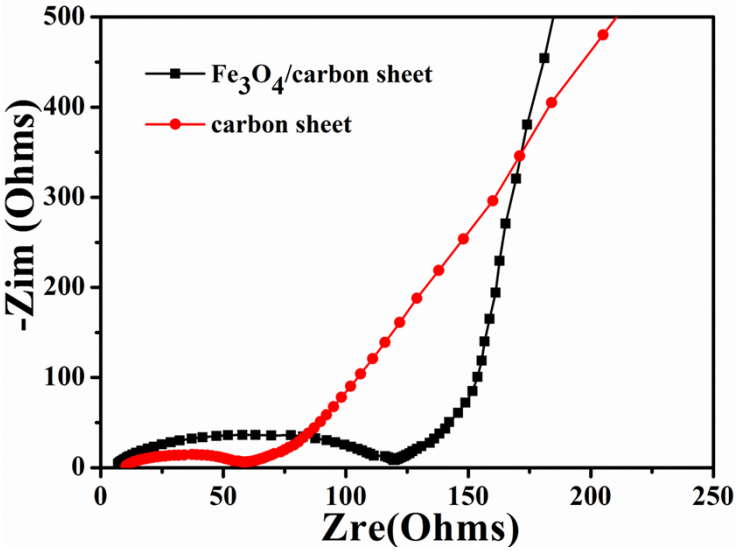

Fig. S8 Nyquist plots of the boron-doped carbon sheet and Fe_3O_4/ boron-doped carbon sheet composites.

Electrochemical impedance spectroscopy (EIS) was carried out on the anode materials after the coin cell was discharged and charged for 2 cycles, meanwhile the SEI film should be formed. The amplitude of 5 mV *versus* the open circuit potential and the frequency range of 0.01 Hz-100 kHz were set for the EIS measurement. The high frequency semicircle in the EIS can be attributed to the resistance of the electrolyte. The middle frequency semicircle corresponds to the charge transfer resistance arising from the charge transfer through the electrode-electrolyte interface. The sloping line at low frequency is known as Warburg impedance, which is due to the lithium ions diffusion/transport in the electrolyte to the electrode surface.[1-7] Apparently, the diameter of the semicircle for carbon sheets electrode in the high-medium-frequency region is significantly smaller than that of Fe_3O_4/boron-doped carbon sheet composite. This indicates that carbon sheet electrodes possess lowest contact and charge-transfer impedances, which can lead to rapid electron transportation during the electrochemical process. The slope of Fe_3O_4/ boron-doped carbon sheet electrodes is higher than that of carbon sheet electrodes in the low-frequency region suggesting that the faster ion diffusion in the Fe_3O_4/ boron-doped carbon sheet electrodes and thus result in excellent rate performance.

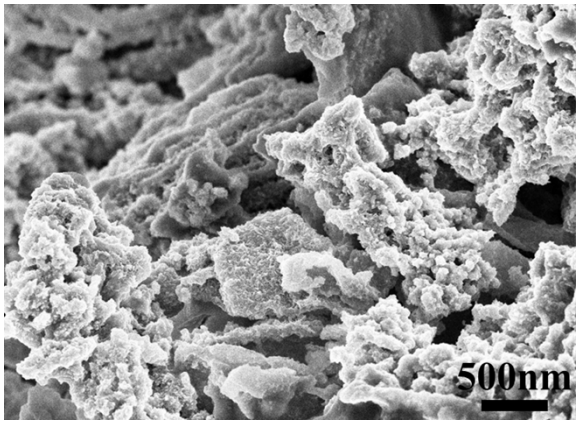

Fig. S9 SEM images of the composite of boron-doped carbon sheets and Fe_3O_4 nanoneedles after 400 cycles' discharging/charging at a current of 100 mA g^{-1}.

1 Y. Dong, R. Ma, M. Hu, H. Cheng, Q. Yang, Y. Y. Li, J. A. Zapien, *Phys. Chem. Chem. Phys*. 2013, 15, 7174.

2 C. Wang, Q. Zhang, Q. H. Wu, T. W. Ng, T. Wong, J. Ren, Z. Shi, C. S. Lee, S. T. Lee, W. Zhang, *RSC Adv.*, 2012, **2**, 10680.

3 Y. Yang, K. Wu, R. Pang, X. Zhou, Y. Zhang, X. Wu, C. Wu, H. Wu, S. Guo, *RSC Adv.*, 2013, **3**, 14016.

4 Y. Yang, R. Pang, X. Zhou, Y. Zhang, H. Wu, S. Guo, *J. Mater. Chem.*, 2012, **22**, 23194.

5 Y. Wang, J. Xu, H. Wu, M. Xu, Z. Peng, G. Zheng, *J. Mater. Chem.*, 2012, **22**, 21923.

6 Y. Xiao, S. Liu, F. Li, A. Zhang, J. Zhao, S. Fang, D. Jia, *Adv. Funct. Mater.*, 2012, **22**, 4052-4059.

7 X. Yang, J. Zhu, L. Qiu, D. Li, *Adv. Mater.*, 23 (2011) 2833-2838.